ISSN: 0975-8585

Research Journal of Pharmaceutical, Biological and Chemical Sciences

Corrosion Mitigation of X-60 type Carbon Steel in Petroleum Formation Water under High Pressure of CO_2

Al-Sabagh AM [1], Migahed MA[1], Mishrif MR[1], Abd-El-Bary HM [2], Mohamed ZM[3], and Hussein BM*[4].

[1] Egyptian Petroleum Research Institute (EPRI), Nasr City, Cairo, Egypt.
[2] Faculty of Science, Al-Azhar University, Nasr City, Cairo, Egypt.
[3] EGPC, Palestine Street part 4, New Maadi, Cairo, Egypt.
[4] Egas Company, Nasr City, Cairo, Egypt .

ABSTRACT

During oil production process, tubing steel immersed in oil wells produced water are exposed to high pressure of CO_2 and this leads to increase their corrosion susceptibility. The present study is aimed to study the corrosion behavior of tubing steel exposed to formation water saturated with CO_2 at varies temperatures in the absence and presence of newly synthesized nonionic surfactants, using electrochemical impedance and potentiodynamic polarization techniques. Surface analytical techniques (SEM and EDS) were used to study the thickness of the adsorbed surfactants molecules on carbon steel. Surface active properties such as surface excess concentration (Γmax), the area per molecule at interface (Amin), and the effectiveness of surface tension reduction were determined from the adsorption isotherms of the prepared surfactants. The results of polarization measurements indicated that the selected surfactants act as mixed type inhibitors in formation water saturated with CO_2. The inhibition efficiency (IE) is dependent upon inhibitor concentration and the number of ethylene oxide unites. It was found that, the charge transfer resistance (R_t) on carbon steel was increased with increasing the inhibitor concentration indicating that the corrosion process is mainly controlled by charge transfer reaction. Quantum chemical parameters such as $E_{HOMO,}$ $E_{LUMO,}$ ΔE, ΔN were calculated discussed.

Keywords: Corrosion in carbon dioxide, Inhibitors, Carbon Steel, Formation water, Polarization, Surface analysis, Surfactants.

Corresponding author

ISSN: 0975-8585

INTRODUCTION

Corrosion of steel by CO_2 has been one of the major problems in the oil industry since 1940. Recently , it has again come to the fore because of the technique of CO_2 injection for enhanced oil recovery and exploitation of deep natural gas reservoirs containing carbon dioxide [1].Crude oil and natural gas can carry various high-impurity produces which are inherently corrosive. In the case of oil and gas wells and pipelines, such highly corrosive media are carbon dioxide (CO_2), hydrogen sulfide (H_2S), and free water [2]. Carbon dioxide (CO_2) corrosion is a great concern in the oil and gas industry [3-4].Up to now, corrosion inhibitor injection is still the most cost-effective method to solve the problem. Among various types of corrosion inhibitors, surfactants have been proved to be effective in controlling CO_2 corrosion [5-7].

Corrosion is the destructive attack of a material by reaction with its environment [8] and a- natural potential hazard associated with oil and gas production and transportation facilities [9]. Almost any aqueous environment can promote corrosion, which occurs under numerous complex conditions in oil and gas production, processing, and pipeline systems [10].The costs attributed to corrosion damages of all kinds have been estimated to be of the order of 3% to 5% of industrialized countries' gross national product [11-13].The total annual cost of corrosion in the oil and gas production industry is estimated to be $1.372 billion, broken down into $589 million in surface pipeline an d facility costs, $463 million annually in down hole tubing expenses, and another $320 million in capital expenditures related to corrosion [14]. Corrosion costs the oil and gas industry tens of billions of dollars in lost income and treatment costs e very year [15]. Corrosion costs US industries alone an estimated $170 billion a year in which the oil and gas industry takes more than half of these costs [16]. Internal corrosion in wells and pipelines is influenced by temperature, CO_2 and H_2S content, water chemistry, flow velocity, and surface condition of the steel [17]. Having a greatly reduced corrosion rate (mm /year) can dramatically increase component life, which leads to much greater benefits such as reduced maintenance costs. Currently, many components used for oil and gas extraction are made from carbon steel - based alloys.

Carbon dioxide corrosion is one the most studied form of corrosion and major problems in oil and gas industry. In the light of common and expensive problems occurring in the oil and gas industry, CO_2 corrosion has been extensively studied in the past few decades. This is generally due to the fact that the crude oil and natural gas from the oil reservoir / gas well usually contains some level of CO_2 with CO_2 corrosion in oil and gas industry is that CO_2. The major concern corrosion can cause failure on the equipment especially the main down hole tubing and transmission pipelines and thus can disrupt the oil/gas production.

Control of internal corrosion of carbon steel pipeline can be achieved by the injection of corrosion inhibitors [18].Corrosion inhibitors are surface active compounds that, in small quantities (ppm level), produce a reduction in metal loss due to corrosion. Vast majority of corrosion inhibitors are made up of molecules which are composed of separate hydrophilic head and hydrophobic tail. It is this combined hydrophilic/hydrophobic nature that causes an inhibitor to partition between oil and water phases in pipe flow.

The basic CO_2 corrosion reaction mechanisms have been well understood and accepted by many researchers through the work done over the past few decades. Sweet corrosion, also called CO_2 corrosion, is major chemical reactions include CO_2 dissolution and hydration to form carbonic acid as shown in equations (1) and (2),

$$CO_2\,[g] \leftrightarrow CO_2\,[aq] \quad (1)$$

$$CO_2\,[g] \leftrightarrow CO_2\,[aq] \quad (2)$$

CO_2 corrosion was also referred to as “acid corrosion” due to the major chemical reaction includes CO_2 and hydration to form a weak carbonic acid in two steps as in equations (3) and (4),

$$H_2CO_3\,[aq] \leftrightarrow H^+ + HCO^-_3 \quad (3)$$

$$HCO^-_3 \leftrightarrow H^+ + CO^-_3 \quad (4)$$

ISSN: 0975-8585

CO_2 corrosion is an electrochemical reaction with the overall reaction between Steel and water given in equation (5)

$$Fe + CO_2 + H_2O \leftrightarrow FeCO_3 + H_2 \quad (5)$$

Thus,CO_2 corrosion leads to the formation of a corrosion product, $FeCO_3$, which when precipitated could form a protective or a non protective scale depending on the environmental conditions **[19]**.The electrochemical reactions at the steel surface include the anodic dissolution of iron as given in equation (6)

$$Fe \leftrightarrow Fe^{+2} + 2e^- \quad (6)$$

The cathodic reactions are proton reduction reaction and the direct reduction of carbonic acid as in equations (7) and (8)

$$2H^+ + 2e^- \rightarrow H_2 \quad (7)$$

$$H_2CO_3 + 2e^- \leftrightarrow H_2 + 2HCO^-_3 \quad (8)$$

Despite more than three decades of intense research, it is still not known which of the two reactions (7) and (8) actually occur on the metal surface. Hence, the net cathodic current was assumed to be the sum of the currents of the two cathodic reactions. It has been suggested that the direct reduction of bi carbonate ion becomes important at higher pH [20].

EXPERIMENTAL

Synthesis of Surfactant Corrosion Inhibitors

The first step was done by reacting one mole of maleic anhydride with one mole of oleic acid to produce the adduct as dark brown liquid and denoted as (MOA) for maleic anhydride- oleic acid adduct [10]. Three ethoxylated hexadecyl amines with different ethylene oxide units (15, 25 & 35) were prepared in the second step [21-22].The ethoxylated product is appeared as a brown viscous liquid, named as ethoxylated Hexadecyl amine ($E_{15}H$, $E_{25}H$ and $E_{35}H$,).Finally Esterification of (MOA) maleic anhydride – oleic acid adduct from the first step with the ethoxylated hexadecyl amine ($E_{(x+y)}H$) [23] from the second step to produce the studied inhibitors I, II and III. The overall scheme of reaction is shown in **Fig.1.**

Chemical composition of the investigated carbon steel alloy

The working electrodes were machined out from commercial carbon steel grade X65.The surface preparation was carried out by grinding/polishing with 1200 grit of silicon carbide paper then degreasing with iso-propanol to remove any dust and scratches so that only the corrosion examined is that which occurred in the cell, and the chemical composition is listed in **Table 1.**

Table 1: Chemical composition of carbon steel alloy

Element	C	Si	Mn	P	S	Ni	Cr	Mo	V	Cu	Al	Fe
Content (Wt %)	0.09	0.22	1.52	0.01	0.05	0.04	0.02	0.004	0.002	0.02	0.04	Rust

Deep oil formation water

The formation water used in this study was supplied from Khalda-Apache "KPC" Petroleum Company, Moghra Zone, Salam Field, Western Desert, Egypt. Most oil and gas field water contains a variety of dissolved organic and inorganic compounds, The Chemical composition of the formation water used in this paper and its physical properties are listed in **Table 2.**

ISSN: 0975-8585

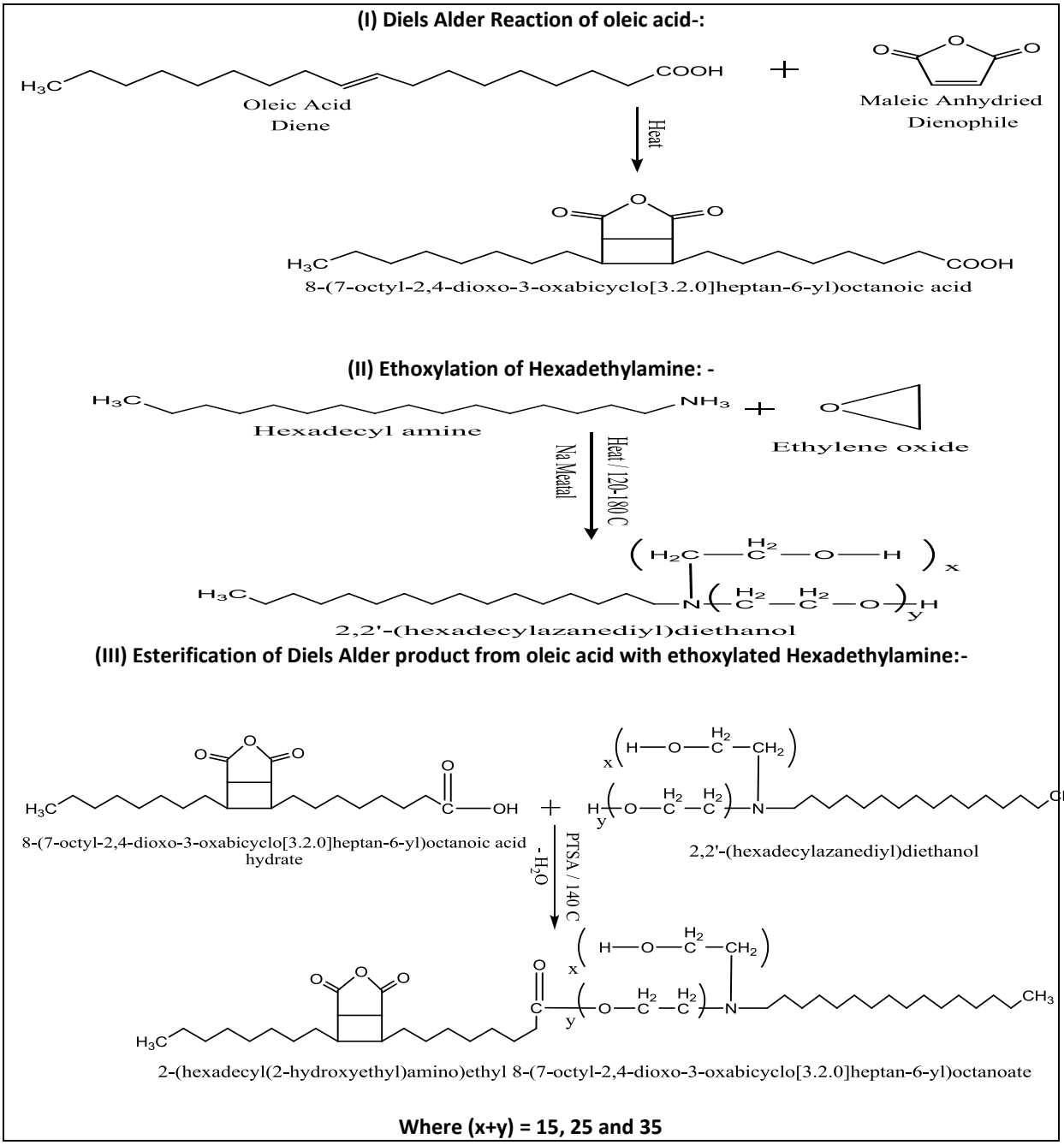

Scheme 1 of surfactant inhibitors preparation

Table 2: Chemical composition and Physical properties of deep oil well formation water used in this investigation

Test	Density g/cm^3	Turbidity NTU	Iron (mg/l)	Total hardness(mg/l)	Sulphate (mg/l)	Salinity as NaCl (mg/l)	Conduc.@ 25 °C µs/cm
Result	1.0199	745	2.2	2714	920	30694	76.5
Test	Chloride (mg/l)	Bi-carbonate (mg/l)	PH	Phosphate (mg/l)	Carbonate (mg/l)	Barium (mg/l)	Cupper (mg/l)
Result	18227	550	6.69	340	Nil	Nile	Nil
Test	Calcium (mg/l)	Magnesium (mg/l)	Zinc (mg/l)	Potassium (mg/l)	T.D.S. (mg/l)	———	———
Result	810	193	0.35	1450	35250	———	———

Structure confirmation of the prepared Surfactants inhibitors

FTIR spectra were analyzed with a Nicolet FTIR spectrophotometer using KBr in a wave number range of 4000–500 cm^{-1} with a resolution accuracy of 4 cm^{-1} all samples were ground and mixed with KBr and then pressed to form pellets. The ADSA-100 analysis required accurate density measurements, which were measured as functions of temperature and nanogels concentration with an AP Paar DMA45 MC 1296 densitometer. Pendent drops were formed on the tip of a Teflon capillary with an outside diameter of 0.1 in. and inside diameter of 0.076 in.

Surface Active Properties for nonionic inhibitors

Surface tension is measured for different concentrations of the synthesized nonionic surfactants dissolved in distilled water at 30 ºC. The measured values of (γ) are plotted against lnC of the surfactant concentration; the intercept of the two straight lines designates the critical micelle concentration where saturation in the surface adsorbed layer takes place. The surface active properties of the surfactant, effectiveness (π_{cmc}), maximum surface excess (Γ_{max}) and minimum area per molecule (A_{min}) were calculated and discussed [24].

Electrochemical Measurements

Electrochemical open circuit potential (OCP) is carried out in acidic media. The electrode is immersed in test solution at OCP for 30 minutes at room temperature to be sufficient to attain a stable state. The polarization curves are measured by scanning rate at 1mV s-1 in range ±0.25 V in both cathodic and anodic potentials to investigate the polarization behavior. All experiments are performed at 40 ºC. Potentiodynamic polarization curves are obtained by changing the electrode potential automatically from -1.2 to -0.4 Vvs.SCE. Electrochemical impedance spectroscopy (EIS) is carried out at OCP in the frequency range of 100 kHz 10 MHz using 10 mV peak-to-peak voltage excitation, An AC sinusoid ±10 mV is applied at the corrosion potential (E_{corr}) [25-26].

Surface analysis properties of carbon steel

The scanning electron microscope (SEM) is a type of electron microscope that images the sample surface by scanning it with a high energy beam of electrons in a raster scan pattern. EDX system attached with a JEOL JSM-5410 scanning electron microscope is used for elemental analysis or chemical characterization of the film formed on carbon steel surface.

RESULTS AND DISCUSSION

The Diels-Alder reaction is one of the most important C-C bond forming organic synthesis reactions in a one-step reaction it enables the regio- and stereoselective construction of five, six and seven membered carbocycles and heterocycles **[27]**.There is only few examples of this cycloaddition are described for unsaturated fatty acids. The reaction is based on converting of un conjugated fatty acids, such as oleic acids, which have been converted into conjuenic acid by conjugation of the double bonds undergoes Diels-Alder reactions at high temperature with dienophiles bearing electron withdrawing groups**[28]**.Not reported yet are Diels-Alder cycloaddition reactions of malice anhydride as dienes and fatty acid derived dienophiles. In this respect, the present work aims to prepare nonionic surfactants from Diels-Alder reaction between modified rosin ester and fatty acid. These extensions of the Diels- Alder reaction with unsaturated fatty acids are addressed in this contribution. The Diels-Alder addition of oleic acid with malice anhydride without any solvent at 150 ºC under nitrogen yielded the Diels–Alder adduct after a reaction time of 2 h in an isolated yield of 78% **(Scheme 1)**. The compounds was separated from the reaction mixture by column chromatography and recrystallized from petroleum ether/diethyl ether (4:1).

ISSN: 0975-8585

Structure confirmation of the synthesized inhibitors

FTIR spectroscopy

FTIR spectrum confirmed the expected functional groups in the synthesized nonionic surfactant showed the following absorption bands. The absorption peaks centered at 1770 and 1851 cm^{-1} are the two characteristic bands which correspond to the absorption of C=O of the anhydride groups in the unreacted cyclic five-membered ring. The stretching absorption bands at 2900 and 2880 cm^{-1} are assigned to v_s and v_{as} of the alkyl group. The peak at 1050cm^{-1} is due to the ethereal band (C-O) $_{stretching}$. It is clear that as ethylene oxide increase, the ethereal band intensity increase. The peak at 1250 cm^{-1} shows the C-N $_{stretching}$. The band at 3435 cm^{-1} is for the terminal OH stretching group of the ethylene oxide unites. FTIR spectrum of the synthesized inhibitor is shown in **Fig.1.**

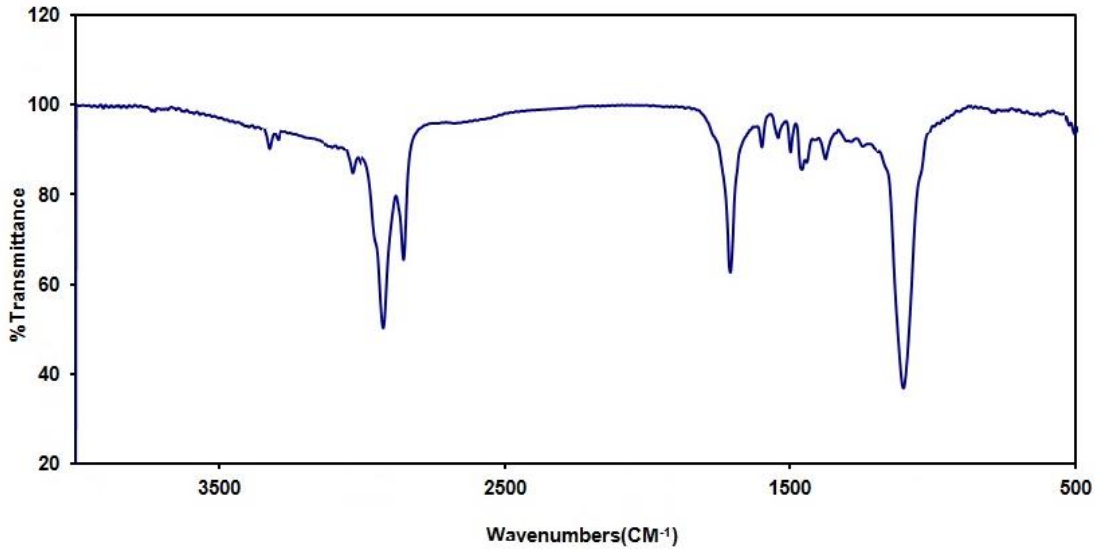

Figure 1: Finger Print for FTIR Spectra of Inhibitor III

Relationship between Critical Micelle Concentration and Degree of Ethoxylation of the Synthesized Surfactants

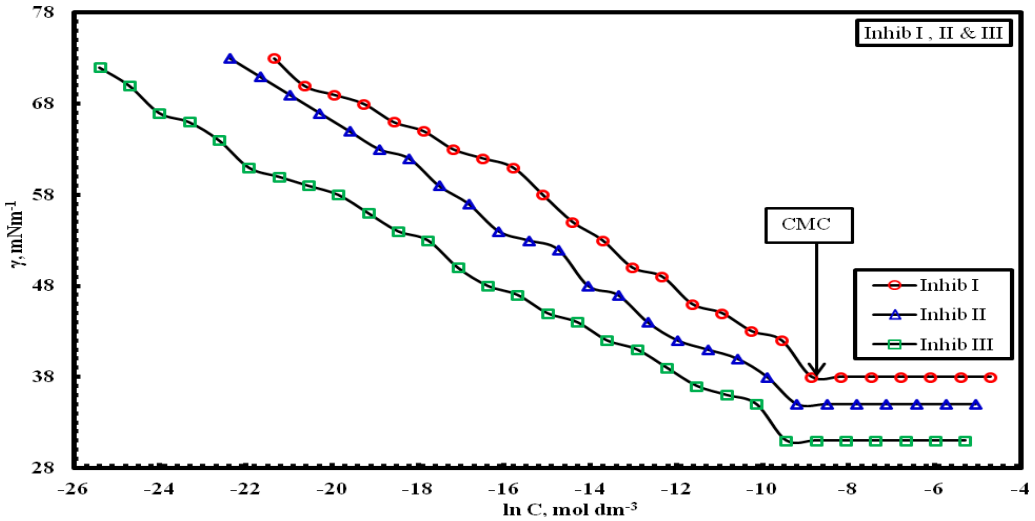

Figure 2: Surface Tension γ - ln C Adsorption Isotherm for investigated inhibitors at 30 ºC

The CMC values of the synthesized surfactants are determined at 30 ºC from the change in the slope of the plotted data of surface tension (γ) versus the natural logarithm of the solute molar concentration.

ISSN: 0975-8585

Surface tension measurements of the synthesized surfactants are shown in **Fig.2.** The presented curves are used for estimating surface activity and confirming the purity of the studied surfactants. It is of interest to mention that all the obtained isotherms showed one phase, which is considered as an indication of the purity for the prepared surfactants. The critical micelle concentration (CMC) is the point in concentration at which it becomes thermodynamically favorable for surfactant molecules in solution to form aggregates (micelles) in order to minimize interaction of either their head groups or their tail groups with the solvent. For the under investigated surfactant, micellization is due to entropic considerations. Water molecules in close proximity to the hydrophobic group of the surfactant molecules take on a certain ordered configuration, which is entropically unfavorable. Once the surfactant concentration reaches a certain level (CMC), the water structure forces aggregation of the hydrophobic tail groups-thus forming surfactant micelles. These plots show that, the surfactant is molecularly dispersed at low concentrations leading to a reduction in surface tension. This reduction increases as the concentration of the surfactant increases. At higher concentrations, however, when a certain CMC is reached the surfactant molecules form micelle, which are in equilibrium with the free surfactant molecules. This is clear in **Fig.2.**

As the concentration of surfactant molecules approaches the CMC, micelles are formed in solution, and similar aggregate structures such as bilayers and multilayers form on the surface **Fig.3.** Further increase in surfactant concentration above the CMC results in other types of aggregates such as lamellar structures and rod-like micelles that can form in solution as well as analogous bilayers or multilayers that form at interfaces [29-30].

Table 3: Surface Active Properties for Investigated Inhibitors at 30 ºC

Surfactants	γcmc.mNm^{-1}	CMC x 10^{4} mol.dm^{-3}	Π cmc. mNm^{-1}	Γ max x 10^{10} mol.cm^{-2}	Amin (nm molecule^{-1})
I	38	1.36	34.3	1.27	131.16
II	35	0.90	37.3	1.11	148.84
III	31	0.68	41.3	0.93	178.74

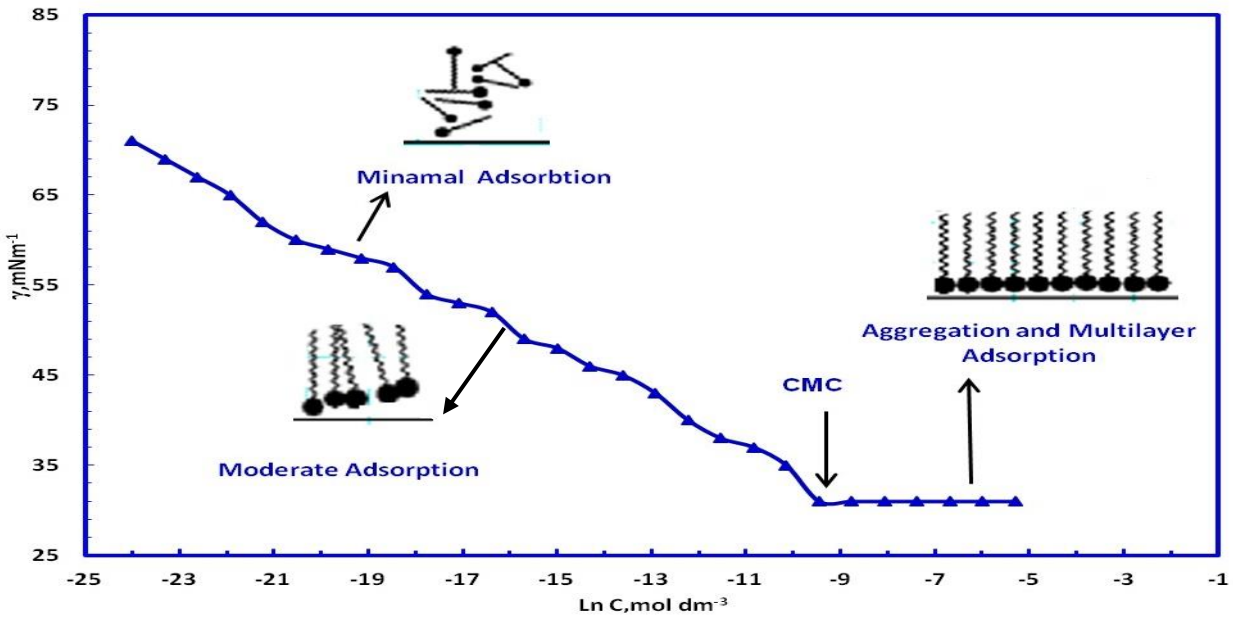

Figure 3: Change of Surface Tension γ-ln C with the concentration of the synthesized inhibitors at 40 ºC.

The values of CMC and the surface tension at CMC (γ_{CMC}) are listed in **Table 3**. By careful inspection of the surface tension values, it can be concluded that, the values decrease be increasing the hydrophilic group from 15 to 35 ethylene oxide units due to the increase in the functional group which enhances the adsorption at the interface. The hydrophobic group tends to expel the surfactant molecules from the solution and

enhance their departure to the interface to get away from the hydrophilic water media. The effectiveness (π_{cmc}) increased as the result of accumulating the surfactant molecules at the interface. The adsorption effectiveness of the prepared surfactants expressed by the maximum reduction of surface tension which was calculated from the equation:

$$\Delta\gamma = \gamma_{water.} - \gamma_{cmc} \qquad (11)$$

The concentration of the prepared surfactants at the solvent-air interface, Γ_{max}, and the area per molecule at the interface, A_{min} were calculated and listed in **Table 3**.The surface excess concentration of the prepared surfactants at the interface can be calculated from the surface or interfacial tension data [31] using the following equation.

$$\Gamma_{max} = 1/RT \pm (-\partial\gamma / \partial \ln c) T \qquad (12)$$

Where $(-\partial\gamma / \partial \ln c) T$ is the slope of the plot of γ versus lnc at constant temperature (T), and R is the gas constant (in J mol^{-1} K^{-1}).Γ_{max} values were used for calculating the minimum area (A_{min}) at the aqueous–air interface. The area per molecule at the interface provides information about the degree of packing and the orientation of the adsorbed surfactants, when compared with the dimensions of the molecules obtained from models. From the surface excess concentration, the area per molecule at the interface is calculated using the equation:

$$A_{min} = 10^{16}/N\,\Gamma_{max} \qquad (13)$$

Where N is Avogadro's number, the area occupied at the interface is increased [31]. The maximum surface excess (Γ_{max}) is expressed as the concentration of surfactant molecules at the interface per unit area, It is clear in **Table 3 and Fig.3**, that the increase of hydrophilic moiety length of surfactant molecules, shift Γ_{max} to lower concentrations. The effectiveness values as well as the maximum surface excess considered as a clear description for the accumulation extent of amphiphiles molecules at the air–water interface. Decreasing the maximum surface excess values indicates the decreasing of the adsorbed molecules at the interface, hence the area available for each molecule will increase. A_{min} increased by increasing the hydrophilic moiety. Since, the molecular weight increases and the availability of the surfactant to be adsorbed on the interface per molecule will decrease. In other words, the larger the molecule, the larger the area occupied per molecule. Hence, small numbers of these surfactants will be needed to be occupied to give the best active properties.

Free Energy of Micellization

By using the values of CMC obtained in **Table 2**, ΔG_{mic} values are listed in **Table 4**.The free energy changes of micellization and adsorption showed negative sign showing the spontaneity of the two processes at 30 ºC. The Gibbs free energies of adsorption and micellization, ΔG_{ads} and ΔG_{mic} decrease gradually by the increase in the number of ethylene oxide groups. This may be due to the increase of hydrophilic moiety of surfactant molecule which enhances the adsorption and micellization at the interface [32]. It is clear that, the negativity of ΔG_{ads} and ΔG_{mic} increase with increasing the hydrophilic group. That is because the hydrophilic group in the amphiphile will be larger and the large hydrophobic group will push it to the interface to be adsorbed at large area per molecule from the interface at the sites which had greater free energy to be calmed down and be in a stable state. In other words, the increase of hydrophilic moiety of surfactant molecule enhances the adsorption and micellization at the interface.

Table 4: Thermodynamic Properties for Investigated Inhibitors at 30 ºC

Surfactants	$\Delta G_{mic.}$ (KJ mol^{-1})	$\Delta G_{ads.}$ (KJ mol^{-1})	$\Delta G_{mic.} - \Delta G_{ads}$ (KJ mol^{-1})
I	-22.42	-25.13	2.71
II	-23.45	-26.80	3.34
III	-24.18	-28.63	4.45

Moreover, ΔG_{ads} has an obvious increase in negativity than ΔG_{mic}. That showed the higher tendency of these amphiphiles towards adsorption rather than micellization then the adsorption will be

accompanied with micellization at last. The tendency towards adsorption is referred to the interaction between the aqueous phases and the hydrophobic chains which pump the amphiphile molecules to the interface [32].

Evaluation of the Efficiency of Synthesized Surfactants as Corrosion Inhibitors

The aim of this part is to investigate how the synthesized nonionic surfactants inhibit the carbon steel corrosion in the oil wells formation water saturated with CO_2 using different techniques, and to propose the adsorption models of surfactants on carbon steel surface. The electrochemical techniques Potentiodynamic polarization and electrochemical impedance spectroscopy (EIS)] are applied to evaluate the corrosion inhibition parameters. The scanning electron microscope (SEM) and energy dispersive analysis of X-ray spectroscopy (EDX) are applied for studying the surface morphology and elemental analysis or chemical characterization of the film formed on the carbon steel surface

Electrochemical Studies

In this study, two types of electrochemical techniques, potentiodynamic polarization and electrochemical impedance spectroscopy (EIS) are used. These studies are carried out for the synthesized nonionic surfactants as corrosion inhibitors with concentrations (50, 100, 150, 200, 250 and 300 ppm), at different temperatures (40 ºC) in the oil wells' formation water saturated with CO_2 as aggressive media.

Potentiodynamic Polarization Measurements

Cathodic and anodic polarization curves for carbon steel in oil wells' formation water saturated with CO_2 in the absence and presence of various concentrations of the nonionic surfactants are show in **Fig.5.** The inhibition efficiency (IE %) was calculated using the equation 14:**[33-38]**,

$$\mathbf{IE\ \%} = \mathbf{1} - \left[\frac{\mathbf{I_{corr}}}{\mathbf{I^{\circ}_{corr}}}\right] \qquad (14)$$

Where I°_{corr} and I_{corr} are the corrosion current density values without and with inhibitor, respectively. The electrochemical parameters, corrosion current density (I_{corr}), corrosion potential (E_{corr}**),** anodic Tafel slope (β_a) and cathodic Tafel slope (β_c), associated with polarization measurements and the inhibition efficiency (IE %) at different inhibitor concentrations are listed in **Table 5**. It is obvious from **Fig. 4 and Table 5** that, according to I_{corr} and IE % values, the inhibitive properties of the studied surfactant inhibitor followed the order/;

Inhib III > Inhib II > Inhib I

The surfactant molecules have the ability to inhibit both anodic and cathodic reactions because Tafel lines are shifted to more negative and more positive potentials with respect to the blank curve by increasing the concentration of the inhibitor. So they act as mixed type inhibitors [39]. This means that the inhibitors have significant effects on retarding both the cathodic reaction and inhibiting the anodic dissolution of carbon steel, [32].This behavior supports the adsorption of inhibitor onto metal surface and caused a barrier effect for mass and charge transfer for anodic and cathodic reactions [40]. Lower corrosion current densities (I_{corr}) are observed with increasing the concentration of the nonionic surfactants inhibitors with respect to the blank without nonionic surfactants inhibitors [32, 41-42].

ISSN: 0975-8585

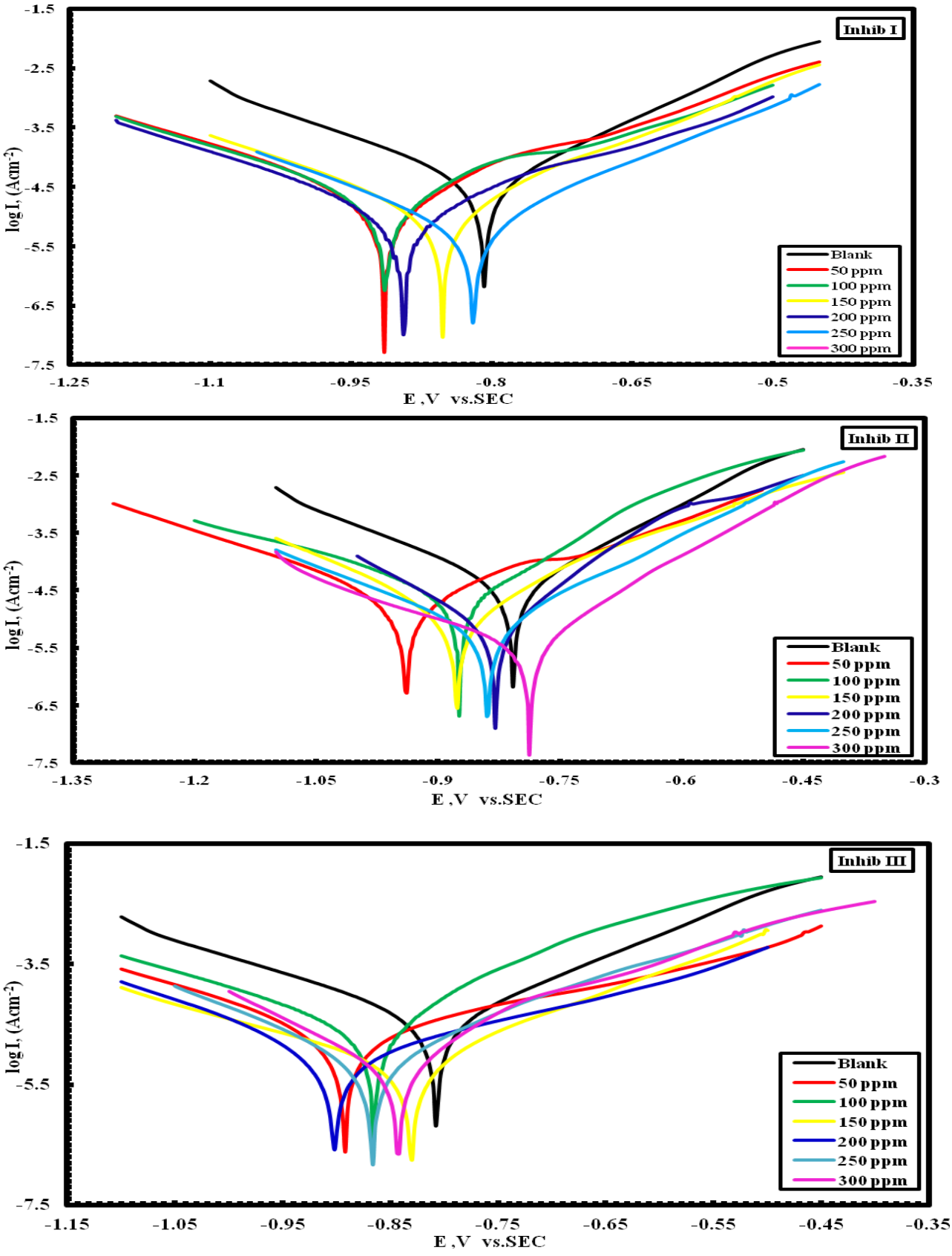

Figure 4: Potentiodynamic polarization curves for the carbon steel in oil wells' formation water saturated with CO_2 in absence and presence of various concentrations of investigated inhibitors (I, II & III) at 40 ºC.

ISSN: 0975-8585

Obtain the results showed that ethoxylation of Hexadecyl amine (E_nH) with 15,25 and 35 degrees , then etherifying the ethoxylated amine with the Diels Alder product adduct (MOA) causes a decrease in the current density due to the newly existence of oxygen which increased as the degree of ethoxylated unite increased. Hence, the inhibitor effect is to reduce the current density to lower values (lower corrosion rate) as a result of increasing the function group which help in attaching the metal surface. The results can be attributed to the different in the molecular structure of both inhibitors.

The value of inhibition efficiency in **Table 5** is increased with increasing the inhibitor concentration from 50 ppm to 300 ppm while the maximum value of (EI %) is obtained for Inhibitor (Inhib III) [40-42]. It is clear that the corrosion current densities (i_{corr}) decrease with increasing inhibitor concentration. The effect was maximal for the concentration 300ppm, which is the optimum concentration of inhibitor required to achieve the efficiency (87%) This could be explained on the basis of inhibitor adsorption on the metal surface and the adsorption process enhances with increasing inhibitor concentration [42].**Table 5** show the values of cathodic Tafel slope (β_c) and anodic Tafel slope (β_a) of surfactants are found to change with inhibitor concentration indicating that the inhibitors controlled both the two reactions[40,43]. In other words, the inhibitors decrease the surface area for corrosion without affecting the mechanism of corrosion and only cause inactivation of a part of the surface with respect to the corrosive medium **Table 5.** Indeed, accurate evaluation of Tafel slopes by Tafel extrapolation is often impossible, simply because an experimental polarization curve does not exhibit linear Tafel regions [32, 44].

Table 5: Electrochemical polarization parameters for the corrosion of carbon steel in the oil wells' formation water saturated with CO_2 in the absence and presence of various concentrations of investigated inhibitors at 40 ºC

Inhibitor	Conc.	$-E_{corr.}$ (mV vs. SCE)	$I_{corr.}$ (µA/cm²)	R_p (K ohm.cm^2)	β_a (mVdec^{-1})	β_c (mVdec^{-1})	IE(%)
I	Blank	-833.4	39.9	1.24	311.6	-108.6	-----
	50	-917.0	26.1	2.47	208.2	-214.7	34.6
	100	-916.3	20.8	2.20	161.9	-183.1	47.9
	150	-924.3	17.1	2.47	183.5	-167.0	57.1
	200	-855.7	12.5	3.33	154.5	-191.0	68.7
	250	-904.6	8.8	3.65	151	-166.2	77.9
	300	-825.0	7.5	3.99	113.8	-188.9	81.2
II	50	-942.6	24.1	2.11	145.8	-255.8	39.6
	100	-877.1	18.9	1.32	122.4	-168.2	52.6
	150	-880.2	15.1	3.18	161.0	-168.9	62.2
	200	-920.5	10.3	3.51	169.9	-160.5	74.2
	250	-832.9	7.9	3.59	100.3	-135.4	80.2
	300	-842.5	6.2	4.95	141.9	-179.6	84.5
III	50	-869.0	22.2	1.25	99.0	-158.3	44.4
	100	-924.3	17.7	2.47	183.5	-167.0	55.6
	150	-905.4	13.8	4.24	185.0	-170.2	65.4
	200	-845.3	8.7	3.44	108.9	-150.8	78.2
	250	-846.4	6.7	3.97	88.9	-113.6	83.2
	300	-814.3	5.1	5.31	115.2	-127.4	87.2

Electrochemical Impedance Spectroscopy Measurements (EIS)

Fig. 5 shows the Nyquist plots of carbon steel immersed in oil wells formation water saturated with CO_2 in the absence and presence of various concentrations of the nonionic surfactants as corrosion inhibitors.

ISSN: 0975-8585

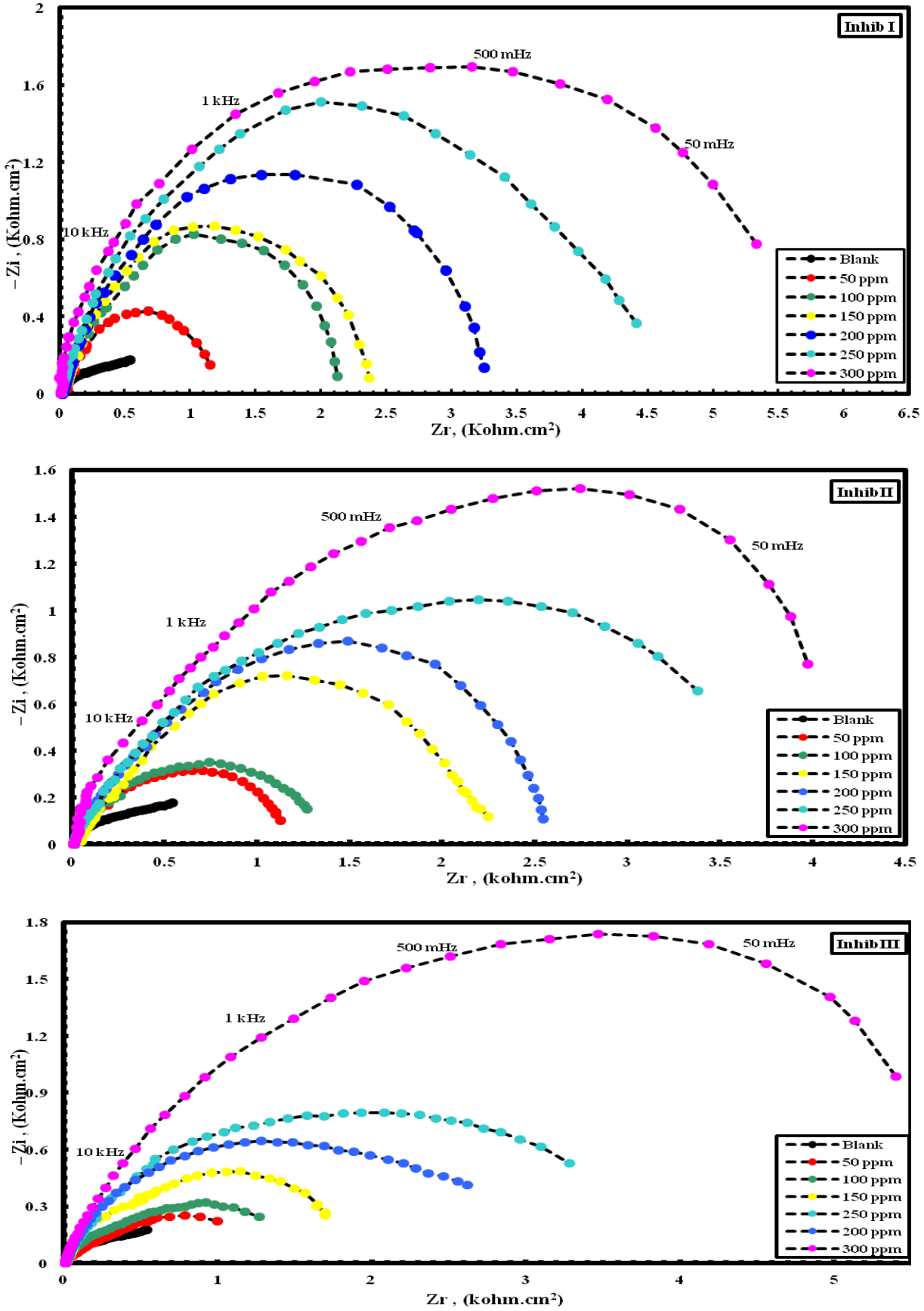

Figure 5: Nyquist plots for carbon steel in oil wells' formation water saturated with CO_2 in the absence and presence of different concentrations of investigated inhibitors at 40 ºC.

ISSN: 0975-8585

Curves have been obtained after 3h of immersion in the formation water saturated with CO_2. It has been reported that the Nyquist plots are generally associated with the charge transfer at the electrode/electrolyte interface [45-46]. EIS data are shown in **Table 6** and the suitable fitted by EIS analyzer equivalent circuit is program and shown in **Fig.5.**

.

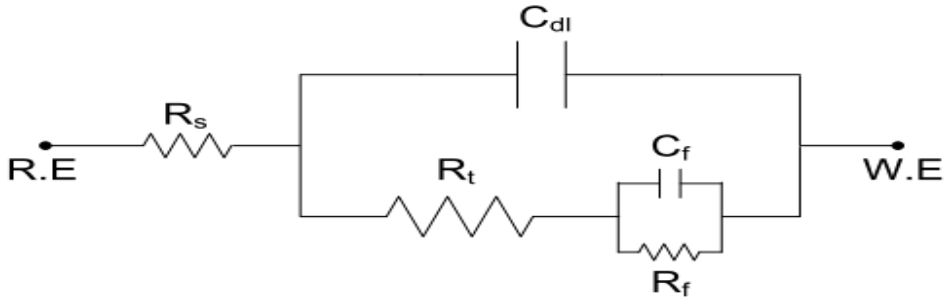

Figure5: Equivalent circuit used to fitting impedance data of carbon steel in formation water at 40 °C saturated with CO_2 environment.

Where R_s is solution resistance, R_f is the film resistance, C_f is film capacitance, C_{dl} is the electrochemical double layer capacitance and finally R_t is the charge transfer resistance. The inhibition efficiency is calculated by charge transfer resistance obtained from Nyquist plots, according to the Eq. (15).

$$IE\ \% = 1 - \frac{R_{t\ Uninhib}}{R_{t\ Inhib}} \qquad (15)$$

$R_{t\ uninhibited\ and}$ $R_{t\ inhibited}$ without and with inhibitor, respectively. Various electrochemical parameters derived from Nyquist plots and IE% values were calculated and listed in **Table5** and listed in **Table 6.** The impedance data indicate that, the values of both (IE %) inhibition efficiency and R_t an increase in charge transfer resistance are found to increase by increasing the inhibitor concentration, while the values of C_{dl} are found to decrease. This behavior can be attributed to a decrease in dielectric constant and / or an increase in the thickness of the electrical double layer, suggests that the inhibitor molecules act by adsorption mechanism at carbon steel / formation water interface [47-48]. The higher the R_t value is, the greater the resistive behavior of the steel, implying a more effective inhibitor. The increase in charge transfer resistance R_t for the inhibited system can be explained by an increase of the resistive behavior of steel owing to the formation of the adsorbed inhibitor molecules on steel surface. Results of EIS data show that (IE %) increases by increasing the inhibitor concentration reaching a maximum value at 300 ppm concentration. The order is in the following direction:

Inhibitor I < Inhibitor II < Inhibitor III

This order is in a good agreement with the data obtained from polarization techniques

Corrosion inhibition mechanism by surfactant molecule

The transition of metal/solution interface from a state of active dissolution to the passive state is of great interest [49].Adsorption of the surfactant molecules occurs because the interaction energy between the surfactant molecules and the metal surface is higher than that between water molecules and the metal surface. So the inhibition effect by surfactants is attributed to the adsorption of the surfactant molecule via their functional groups onto the metal surface. The adsorption rate is usually rapid and hence the reactive metal is shielded from the aggressive environment. Corrosion inhibition depends on the adsorption ability of the surfactant molecules on the corroding surface, which is directly related to the capacity of the surfactant to aggregate to form clusters (micelles). The critical micelle concentration, CMC, is a key factor in determining the effectiveness of a corrosion inhibitor. Below CMC as the surfactant concentration increases, the molecules tend to aggregate at the interface, and this interfacial aggregation reduces the surface tension. Above CMC the metal surface is covered with a monolayer of surfactant molecules and the additional molecules combine to form micelles or multiple layers. This showed in **Fig.3,** consequently, does not alter the surface tension and the corrosion rate [50].

ISSN: 0975-8585

Table 6: Data obtained from electrochemical impedance spectroscopy (EIS) measurements of carbon steel in oil wells' formation water saturated with CO_2 in the absence and presence of various concentrations of investigated inhibitors at 40 ºC.

Inhibitor	Conc.	Rs $\Omega.cm^2$	n_1	R_f $K\Omega.cm^2$	C_f μFcm^{-2}	n_2	Rt $\Omega.cm^2$	C_{dl} μFcm^{-2}	IE %
I	Blank	6.5	0.88	---------	------	0.94	0.75	139.0	------
	50	8.2	0.90	0.026	41.8	0.87	1.16	102.9	35.2
	100	10.4	0.92	0.029	36.2	0.90	1.45	90.7	48.1
	150	12.8	0.95	0.035	31.9	0.85	1.80	81.7	58.3
	200	15.3	0. 84	0.039	22.1	0.79	2.43	71.2	69.2
	250	18.1	0.91	0.041	20.7	0.76	3.57	50.4	78.4
	300	19.3	0.83	0.042	19.8	0.81	4.28	35.2	82.5
II	50	9.3	0.97	0.028	43.2	0.91	1.25	56.6	40.1
	100	10.4	0.96	0.034	37.5	0.80	1.58	50.2	52.6
	150	11.8	0.84	00.41	31.4	0.75	2.01	48.6	62.8
	200	14.5	0.79	0.044	25.2	0.81	2.94	40.5	74.5
	250	17.2	0.83	0.049	23.6	0.92	4.87	36.5	81.6
	300	19.6	0.85	0.052	22.8	0.76	5.03	32.8	85.1
III	50	12.8	0.82	0.033	45.1	0.81	1.37	65.5	45.2
	100	14.3	0.94	0.039	39.3	0.78	1.72	46.2	56.4
	150	15.2	0.85	0.041	33.8	0.91	2.22	38.2	66.2
	200	19.5	0.92	0.046	26.7	0.79	3.59	35.4	79.1
	250	22.3	0.79	0.053	24.9	0.85	4.87	34.9	84.6
	300	25.1	300	0.055	23.5	0.82	6.19	31.1	87.9

Quantum chemical study:

Computational study

Table 7 shows the calculated quantum chemical parameters for inhibitor I) which included, the energy of the highest occupied molecular orbital (E_{HOMO}), the energy of the lowest unoccupied molecular orbital (E_{LUMO}), the energy gap (ΔE), the dipole moment (μ) and logP.

Table 7 Quantum Chemical Parameters of the Investigated Inhibitors

Inhibitor	E_{HOMO} (eV)	E_{LUMO} (eV)	ΔE (eV)	μ (debye)	LogP	Polarizability (Å3)	Hydration energy, E_{hydr}, (k cal mol^{-1})	Surface area, A, (nm^2)	Total energy, E_T, (eV)
I	-6.67	0.236	6.906	4.33	7.45	130.43	-24.45	2449.02	-376037

According to the frontier molecular orbital theory, chemical reactivity can be considered in terms of interaction between the E_{HOMO} and the E_{LUMO}. E_{HOMO} indicates the tendency of a molecule to donate electron while E_{LUMO} indicates the tendency of a molecule to accept a lone pair of electron [51].Therefore, higher value of E_{HOMO} and lower value of E_{LUMO} signify better inhibition efficiency. Careful examination of the experimental results reveals that based on increasing values of E_{HOMO} and on decreasing value of E_{LUMO}. This trend is consistent with results obtained from experiments.

The ΔE of a molecule is defined as the difference between the E_{LUMO} and the E_{HOMO} (i.e $\Delta E = E_{LUMO} - E_{HOMO}$). The ΔE of a molecule is a measure of the hardness or softness of a molecule [52]. Hard molecules are characterized by larger values of ΔE and vice versa. However, hard molecules are less reactive than soft molecules because the larger the gap between the last occupied orbital and the first virtual orbital, the more it is difficult for intermolecular electron transfer to proceeds. From the calculated values of the ΔE, the trend for

the variation of the inhibition efficiency of the studied inhibitor with decreasing value of ΔE is similar to that deduced from experimental data.

μ is the measure of the polarity in a bond and is related to the distribution of electron in a molecule [53]. Although, there are some inconsistencies on the use of μ as a predictor for the direction of a corrosion inhibition reaction, it is generally agreed that the adsorption of polar compounds possessing high dipole moments on the metal surface should lead to better inhibition. Comparison of the results obtained from quantum chemical calculations with orbital experimental inhibition efficiencies indicated that the inhibition efficiencies of the inhibitors increase with decreasing value of μ. Also, it was found that the higher the value of logP, the more hydrophobic is the molecule hence water solubility is expected to decrease with increasing value of logP. From the point of view of corrosion inhibition process, the processes of inhibition that are affected by hydrophobicity are not well established. However, it is most probably that hydrophobicity can be used to predict the mechanism of formation of the oxide/hydroxide layer on the metal surface (which reduces the corrosion process drastically) [54]. From the results obtained, the inhibition efficiency of the studied inhibitors is found to increase with increasing value of logP. This trend supports experimental results.

Fig.9 shows the (HOMO, LUMO) molecular orbitals of inhibitor I or a representation sample in addition to its electrostatic potential.

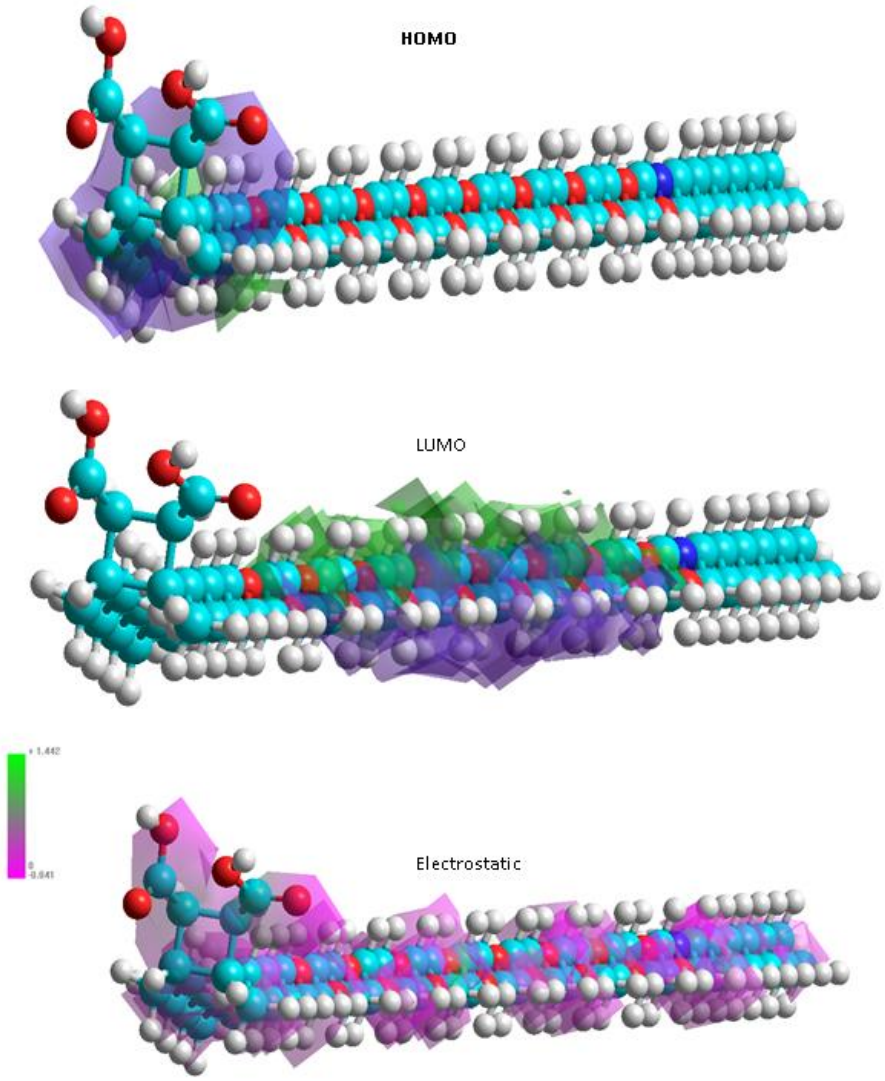

Figure 9: the frontier Molecular orbital density distribution for the investigated inhibitor.

ISSN: 0975-8585

Surface Analysis

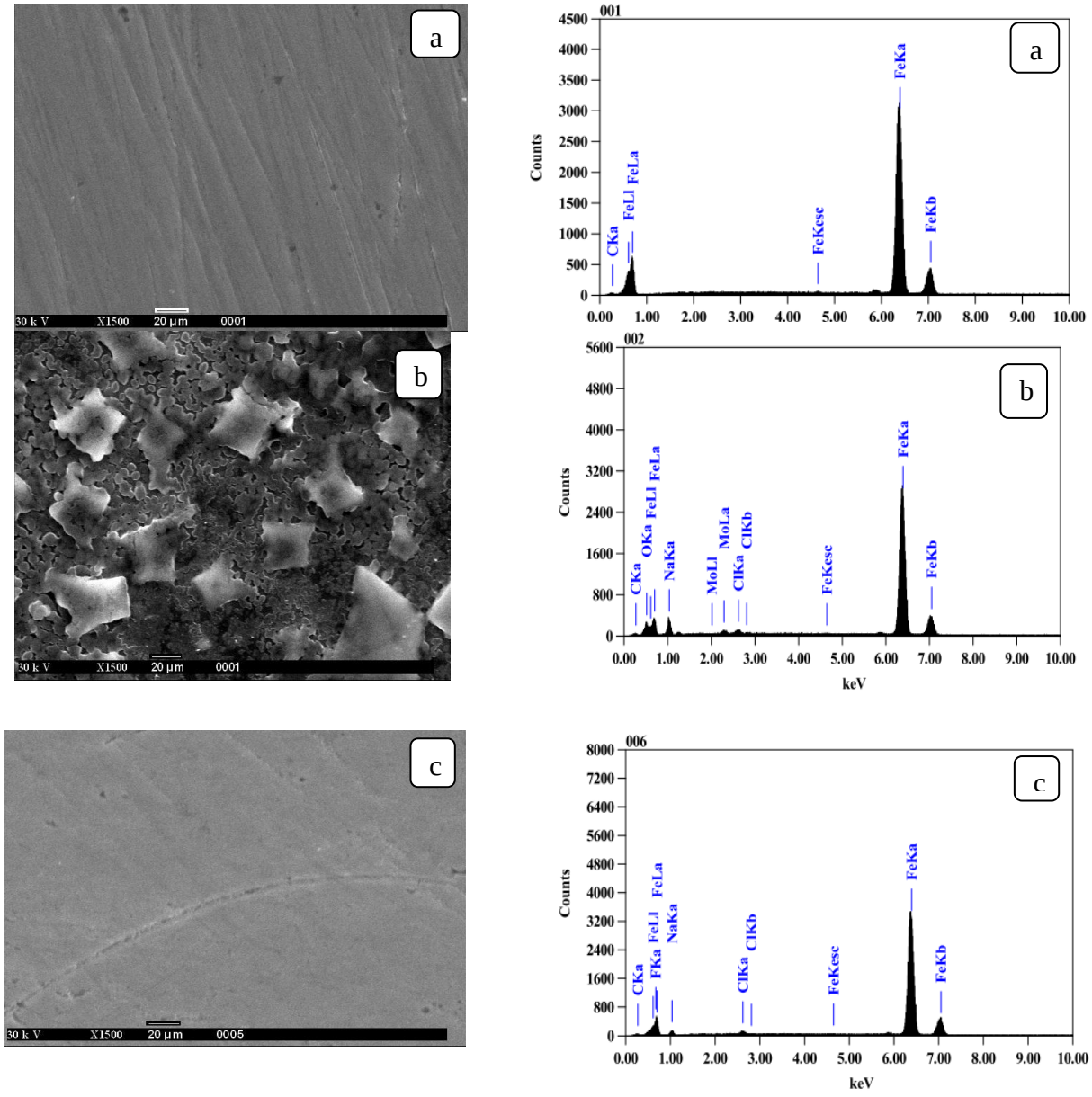

Figure 7: SEM images and EDX for the carbon steel surface: (a) polished sample, (b) after immersion in the oil wells formation water under sour conditions) and (c) after immersion in the oil wells formation water at 40 ºC saturated with CO_2 environment in the in presence of 300 ppm of the best inhibitor (Inhib III).

Fig. 5 (a) shows a characteristic inclusion observed on the polished carbon steel surface, which is probably an oxide inclusion [55], and The EDX spectrum in **Fig.5 (a)** shows the characteristics peaks of some of the elements constituting the polished carbon steel surface. Hence, a comparison can be drawn with the morphology after exposure to the corrosive media. SEM image of the surface and the spectrum of the polished of carbon steel specimen after immersion in the oil wells formation water saturated with CO_2 in absence and presence of 300 ppm of the best inhibitor (Inhib III) for 30 days, are shown in **Fig.6 (b) and (c)** respectively. The resulting scanning electron micrographs reveal that, the surface is strongly damaged and observed as high surface roughness, owing to corrosion in the absence of the inhibitor, but in presence of the inhibitor, there is a much less damage on the surface. This may be attributed to the formation of a good protective film on the carbon steel surface. Hence, the inhibitor (Inhib III) provides good protection for the carbon steel surface against corrosion in the oil wells' formation water saturated with CO_2. The protective film formed on the carbon steel surface in presence of 300 ppm of inhibitor (Inhib III) appears to be very smooth and to cover the

whole surface. This confirms the obtained high inhibition efficiency of inhibitor (Inhib III) from electrochemical measurements at 300 ppm concentration. The spectra of **Fig.3 (c)** show that the Fe peak is decreased considerably relative to the samples in **Fig.6 (a) and (b).** This decreasing of the Fe band indicates that the strongly adherent protective film of inhibitor (Inhib III) is formed on the polished carbon steel surface, which leading to a high degree of inhibition efficiency [55].The appearances of oxygen signal in **Fig.6 (b**) is due to the carbon steel surface exposed to the formation water saturated with CO_2 in the absence of the inhibitor (Inhib III).Therefore, the EDX and SEM examinations of the carbon steel surface support the results obtained from the chemical and electrochemical methods that the synthesized surfactants inhibitors are a good inhibitor for the carbon steel in the oil wells formation water saturated with CO_2.

CONCLUSIONS

1. The critical micelle concentration considers a key factor in determining the effectiveness of surfactants as corrosion inhibitors due to large reduction of surface tension at CMC.
2. The inhibition efficiency percentage of the surfactants increases by increasing the ethylene oxide units of inhibitor molecules.
3. All the investigated nonionic surfactants are effective inhibitors for corrosion of carbon steel in oil wells' Formation water saturated with CO_2.
4. The inhibition mechanism is attributed to the strong adsorption ability of the selected surfactants on carbon steel surface, forming a good protective layer, which isolates the surface from the aggressive environment.
5. The potentiodynamic polarization curves indicated that, the inhibitor molecules inhibit both anodic metal dissolution and also cathodic oxygen reduction, so that the undertaken surfactants classified as mixed type inhibitors.
6. A good correlation was observed between the EIS data and the results of polarization measurements.
7. The formation of a good protective film on carbon steel surface is confirmed using SEM and EDX techniques.

ACKNOWLEDGMENTS

I would like to thank all the staff members and all my friends in **EPRI** and **Egas** Company for their help and support. I would like to express my thanks and gratitude to **Dr. Eman Khames** for helping me in quantum chemistry.

REFERENCES

[1] *P110Steel Investigated by SEM and Electrochemical Technique'*. Iron and steel rese arch International, Year 2009. 16(4): p. 89 -94.
[2] Lusk D, Gupta M, Boinapally K, Cao Y (2008) Armoured against corrosion. Hydrocarb Eng 13:115 – 118
[3] Kermani M. B., Morshed A., *Corrosion*, 2003, *59*(8), 659
[4] Lopez D. A., Perez T., Simison S. N., *Materials & Design*, 2003, *24*(8), 561
[5] Gonzalez-Rodriguez C. A., Rodriguez-Gomez F. J. Genesca- Llongueras J., *Electrochim. Acta*, 2008, *54*(1), 86
[6] Paolinelli L. D., Perez T., Simison S. N., *Corros. Sci*., 2008, *50*(9), 2456
[7] Paolinelli L. D., Pérez T., Simison S. N., *Mater. Chem. Phys*., 2011, *126*(3), 938
[8] Roberge PR (2000) Handbook of corrosion engineering. McGraw -H ill, New York .
[9] Kermani MB, Smith LM (1997) CO_2 corrosion control in oil and gas production: design considerations. The Institute of Materials, European Federation of Corrosion Publications, London.
[10] Champion Technologies (2012) Corrosion mitigation for complex environments. Champion Technologies, Houston.
[11] Corbin D, Willson E (2007) New technology for real-time corrosion detection. Tri-service corrosion conference, USA
[12] Uhlig HH (1949) The cost of corrosion in the United States. Chem and Engng News 27:2764
[13] Lekan Taofeek Popoola, Alhaji Shehu Grema and Adebori Saheed Balogun, Ganiyu . Kayode Latinwo, Babagana Gutti , International Journal of Industrial Chemistry 2013, 4:35.
[14] Champion Technologies (2012) Corrosion mitigation for complex environments. Champion Technologies, Houston.
[15] Simons MR (2008), Report of offshore technology conference (OTC) presentation, NACE International oil

and gas production.
[16] Tuttle RN (1987) Corrosion in oil and gas production. J of Petrol Techno 39:756 –762
[17] http://www.touchbriefings.com/pdf/30/exp032_p_12Nyborg.pdf
[18] L. Smith, "Control of Corrosion in Oil and Gas Production Tubing", British Corrosion Journal, vol 34, pp 247-253, 1999.
[19] Hunnik E.W.J, V., Po ts.B.F.M, and Hendriksen.E.L.J.A, The Formation of Protective $FeCO_3$ Corrosion Product Layers in $CO_2$1996(Paper No.6). Corrosion. Corrosion/96,
[20] Gray LGS, et al. Effect of pH and Temperature on the Mechanism of Carbon Steel Corrosion by Aqueous Carbon Dioxide. Corrosion/90, 1990. Paper No.40 (Houston, TX: NACE International, 1990).
[21] Al-Sabagh, A. M.; Abdul-Raouf, M. E. and Abdel-Raheem, R., Reactivity of polyester aliphatic amine surfactants as corrosion inhibitors for carbon steel in formation water (deep well water), Colloids and Surfaces A: Physicochemical and Engineering Aspects, 251 (2004) 167-174.
[22] Negm,N.A. A.M. et al. El Din Effectiveness of some diquaternary ammonium surfactants as corrosion inhibitors for carbon steel in 0.5 M HCl solution CorrosionScience46(2004)2503–2516
[23] Marco Ormellese, Luciano Lazzari, Sara Goidanich, Gabriele Fumagalli, Andrea Brenna A study of organic substances as inhibitors for chloride-induced corrosion in concrete Corrosion Science 51 (2009) 2959–2968.
[24] Negm.N.A, Ghuiba. F.M, Tawfik. S.M, Novel isoxazolium cationic Schiff base compounds as corrosion inhibitors for carbon steel in hydrochloric acid Corrosion Science 53 (2011) 3566–3575.
[25] Zhang. G.A, Cheng. Y.F, Electrochemical characterization and computational fluid dynamics simulation of flow accelerated corrosion of X65 steel in a CO2 saturated oil field formation water, Corrosion Science 52 (2010) 2716–2724
[26] Gao. M, Pang. X, Gao. K, The growth mechanism of CO2 corrosion product films Corrosion Science 53 (2011) 557–568
[27] Behr. A.; Fiene. M.; Naendrup. F.and Schürmann K., Eur. J. Lipid Sci. Technol., 342 (2000)
[28] Oppolzer W., Intermolecular Diels-Alder Reactions, in: ComprehensiveOrganic Synthesis,Vol. 5, Eds. Trost, B. M., and I.Fleming, Pergamon Press 1991, p. 315.
[29] Miller CA, Qutubuddin , Eike HF, Parfitt CD (E ds), Interfacial Phenomena in polar Media, 'Surfact ant Science Series', Vol. 21, (Marcel Dekker, Inc., New York 1 987), 166.
[30] Rosen MJ, in 'Surfactants and Interfacial Phen omena', (Wiley, New York, 1978), pp. 1–301.
[31] Atta. A M.; Dyab A.K. F. and Al-Lohedan H. A., JSurfactDeterg, 16, 343 (2013)
[32] Negm.N.A, Ghuiba. F.M, Tawfik. S.M, Novel isoxazolium cationic Schiff base compounds as corrosion inhibitors for carbon steel in hydrochloric acid Corrosion Science 53 (2011) 3566–3575.
[33] Migahed MA, Azzam EMS, Al-Sabagh AM, Materials Chemistry and Physics, 2004, 85, 273–279.
[34] Sobramanyam NC, Mayannu SM, J. Electrochem. Soc. India, 1984, 33, 273.
[35] Frumkin AN, Z. Phys. Chem. 1915, 116, 166.
[36] El-Sayed A, J. Appl. Electrochem., 1997, 27, 193.
[37] Abdel Nabey BA, Khamis E, Ramadan MS, El-Gindy A, in: 8th European Symp. Corros. Inhibitors, Ann. Univi. Ferrara N.S. Sez., 1995, 10, 299.
[38] Bentiss. F.; Lagrenee. M. and Traisnel.M.,Corrosion 56 (2000) 733.
[39] Migahed, M.A.; Hegazy, M.A. and Al-Sabagh, A.M., Synergistic inhibition effect between Cu2+ and cationic gemini surfactant on the corrosion of downhole tubing steel during secondary oil recovery of old wells, Corrosion Science 61 (2012) 10-18.
[40] Omanovic. S. and Roscoe. S.G., Corrosion 56 (2000) 684.
[41] Migahed, M.A.; Abd-El-Raouf, M.; et al. Effectiveness of some non ionic surfactants as corrosion inhibitors for carbon steel pipelines in oil fields,Electrochimica Acta,50:24(2005)4683-4689.
[42] Zhang. G.A, Cheng. Y.F, Electrochemical characterization and computational fluid dynamics simulation of flow accelerated corrosion of X65 steel in a CO2 saturated oil field formation water, Corrosion Science 52 (2010) 2716–2724
[43] Hluchan. V.; Wheeler. B.L.and Hackerman. N,Werk, Korro. 39 (1988) 512.
[44] Amin. M.A.; Abd El Rehim. S.S.and Abdel-Fatah. H.T.M., Corros Sci. 51 (2009) 882.
[45] Bentiss .F.; Traisnel. M.; Chaibi. N.; Mernari. B.; Vezin.H.and Lagrenee. M.,Corros. Sci. 44 (2002) 227.
[46] Migahed, M.A.; Mohamed, H.M. and Al-Sabagh, A.M., Corrosion inhibition of H-11 type carbon steel in 1 M hydrochloric acid solution by N-propyl amino lauryl amide and its ethoxylated derivatives, Materials Chemistry and Physics, 80 (2003) 169–175.
[47] El-Sabee, M. Z.; Morsi, R. E. and Al-Sabagh, A.M., Surface active properties of chitosan and its derivatives, Colloids and Surfaces B: Biointerfaces, 74 (2009) 1–16.

ISSN: 0975-8585

[48] Bentiss .F.; Traisnel. M.; Chaibi. N.; Mernari. B.; Vezin.H.and Lagrenee. M.,Corros. Sci. 44 (2002) 227.
[49] Malik MA , Hashim MA, F. Nabi , AL-Thabaiti SA , Khan Z, Int. J. Electrochem. Sci., 2011, 6, 1927 – 1948.
[50] Migahed MA, Abd-El-Raouf M, et al. Electrochimica Acta, 2005, 50, 4683– 4689.
[51] Zhihua Tao, Shengtao Zhang, Weihua Li, Baorong Hou, Corrosion inhibition of mild steel in acidic solution by some oxo-triazole derivatives Corrosion Science 51 (2009) 2588–2595
[52] William.Durnie, Roland.DeMarco,AlanJe.erson,Brian. Kinsella Harmonic analysis of carbon dioxide corrosion Corrosion Science 44(2002)1213–1221
[53] M. Hosseini, H. Tavakoli, T. Shahrabi, J. Appl. Electrochem. 38, 1629 (2008).
[54] Fuchs-Godec, Miomir. G, Pavlovic, Synergistic effect between non-ionic surfactant and halide ions in the forms of inorganic or organic salts for the corrosion inhibition of stainless-steel X4Cr13 in sulphuric acid, Corrosion Science 58 (2012) 192–201.
[55] Migahed, M.A.; et al. Corrosion inhibition of carbon steel in acid chloride solution using ethoxylated fatty alkyl amine surfactants, Journal of Applied Electrochemistry, 36: 4 (2006) 395–402.